Structural Insights into the Conformation and Oligomerization of E2~Ubiquitin Conjugates

Richard C. Page[a,c,*], Jonathan N. Pruneda[b,c], Joseph Amick[a], Rachel E. Klevit[b] and Saurav Misra [a,*]
[a] Department of Molecular Cardiology, Lerner Research Institute, Cleveland Clinic, 9500 Euclid Avenue, Cleveland OH 44195, USA.
[b] Department of Biochemistry, University of Washington, Seattle WA 98195, USA.
[c] These authors contributed equally to this work.
* E-mail: pager2@ccf.org and misras@ccf.org

Supplemental Information

ADDITIONAL EXPERIMENTAL PROCEDURES

Molecular modeling of the Ube2s~Ub conjugate

A molecular model of the the Ube2s~Ub conjugate was generated using HADDOCK (*1*) derived restraints published by Wickliffe *et al.* 2011 (*2*). Starting coordinates for Ube2s residues 6-156 and Ub residues 1-76 were downloaded from the PDB (Ube2s: 1zdn, chain A; Ub: 1ubq). HADDOCK restraints and putative salt bridges (Ube2s-Glu142:Ub-Lys48, Ube2s-Flu51:Ub-Lys6, Ube2s-Glu126:Ub-Arg42 and Ube2s-Asp102:Ub-Arg74) were incorporated as input into a combined rigid body/torsion angle dynamics simulated annealing protocol in Xplor-NIH (*3*). HADDOCK distances were incorporated as ambiguous NOE distances as previously defined (*2*). Salt bridges were included as ambiguous NOE distances between the Ube2s carboxylate oxygen atoms to the Ub amino or guanidine nitrogen atoms with a distance range of 2.0 to 5.0 Å, a typical N-O salt bridge distance range (*4, 5*). For all calculations, the thioester bond between Ub-Gly76-C and Ube2s-Cys95-SG was explicitly defined.

The combined rigid body/torsion angle dynamics smulated annealing protocol began with rigid body minimization where Ube2s was held fixed, Ub was allowed free rotation and translation, and only ambiguous distance restraints (k_{noe}) and van der Waals repulsion (k_{vdw}) terms were included. Next, a round of rigid body dynamics was conducted lowering the bath temperature from 1500K to 500K in 25K increments and exponentially increasing k_{noe} and k_{vdw}. Finally, a round of combined rigid body/torsion angle dynamics lowered the bath temperature from 1500K to 25K in 25K increments while allowing Ube2s and Ub each to freely translate and rotate. The flexible Ub C-terminal tail (residues 70-76) and side chains defined as interfacial residues by Wickliffe *et al.* 2011 (*2*) were allowed to freely sample torsional space during the combined rigid body/torsion angle dynamics cooling phase. The energy terms utilized by the docking protocol consisted of an ambiguous distance restraint term (E_{noe}), a van der Waals repulsion term (E_{vdw}) to avoid steric clashes, a radius of gyration term (E_{gyr}) to minimize expansion of the complex and a torsion angle database energy term (E_{tor}) to favor preferred rotamer conformations for interfacial side chains (*6*). An ensemble of 100 structures was generated and the best structure was selected as the solution with the lowest total energy and no ambiguous distance restraint violations greater than 0.5Å.

Ube2s~Ub molecular contact plots
Cα-Cα Contact distance plots for Ube2s~Ub inter-molecular interactions were calculated using the best Ube2s~Ub model as described in *Experimental Procedures*. Contact distance plots were calculated using the Bio.PDB module within *BioPython* (*7*). The Cα-Cα distance matrices between Ube2s and Ub were plotted as a heat map using *matplotlib* with a distance cutoff of 15 Å.

Structure Validation of the UbcH5c~Ub conjugate
A stereochemical and geometric analysis of the UbcH5c~Ub structure was performed using *MolProbity (8, 9)*. 98.2% of all residues lie within the favored regions of the Ramachandran plot and 100% of residues lie within allowed regions. *MolProbity* analysis of all-atom contacts calculated a clash score of 16.55, ranking the UbcH5c~Ub structure in the 76th percentile of 335 structures at similar resolution. The *MolProbity* score (a weighted measure of stereochemical and geometric statistics) for the UbcH5c~Ub structure was 1.72, which ranks the structure in the 98th percentile of 9,377 structures of similar resolution.

Docking UbcH5~Ub oligomers to full length CHIP
The full length CHIP structure was obtained from PDB ID 2c2l (*10*). An initiating UbcH5~Ub was docked by aligning the UbcH5c from PDB 3ugb and UbcH5b from PDB 3a33 to the UbcH5a molecule of PDB ID 2oxq (*11*). Docking to full length CHIP was completed by aligning the full-length CHIP structure to the CHIP-Ubox domains of PDB ID 2oxq. UbcH5~Ub oligomers were extended by aligning oligomeric UbcH5c~Ub chains (PDB 3ugb) or UbcH5b~Ub chains (PDB 3a33) onto the docked initiating UbcH5.

Docking UbcH5~Ub oligomers to the Cul1-Rbx1-Skp1-Skp2 SCF ligase complex
The structure of the Cul1-Rbx1-Skp1-Fbox^{Skp2} SCF ligase complex was obtained from PDB ID 1ldk (*12*). The structure of Skp2 was obtained from PDB ID 2ass (*13*). The structure of the c-CBL/UbcH7 complex was obtained from PDB ID 1fbv (*14*). Docking of the initiating UbcH5~Ub was carried out by aligning UbcH5c from PDB 3ugb and UbcH5b from PDB 3a33 onto the UbcH7 of the c-CBL/UbcH7 complex (PDB 1fbv). The Cul1-Rbx1-Skp1-Fbox^{Skp2} SCF ligase complex (PDB 1ldk) was then modeled into the UbcH5~Ub/RING complex by aligning the Rbx1 domain of the Cul1-Rbx1-Skp1-Fbox^{Skp2} SCF ligase complex to the c-CBL domain. The structure of Skp2 was introduced by aligning the Fbox of Skp2 to the Fbox^{Skp2} within the Cul1-Rbx1-Skp1-Fbox^{Skp2} SCF ligase complex UbcH5~Ub oligomers were extended by aligning oligomeric UbcH5c~Ub chains (PDB 3ugb) or UbcH5b~Ub chains (PDB 3a33) to the docked initiating UbcH5.

SUPPLEMENTAL FIGURES

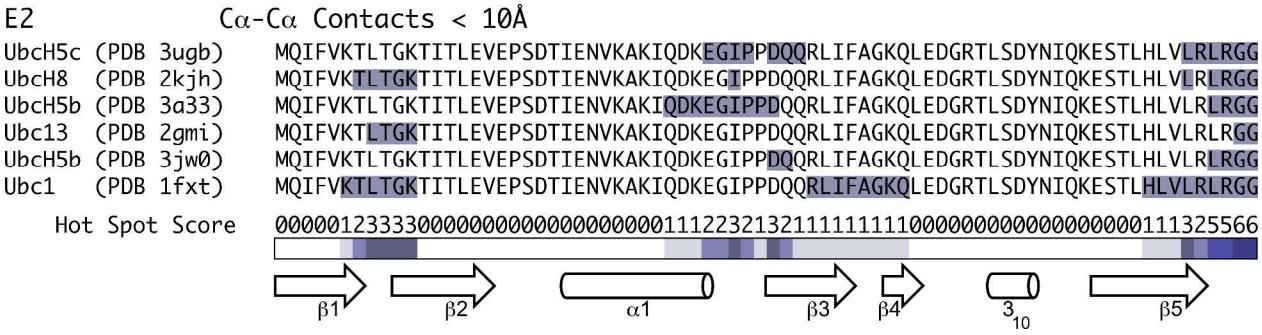

Supplemental Figure S1. Sequence view of intra-conjugate E2/Ub interactions. Ub residues within each E2~Ub structure with Cα-Cα E2/Ub distances less than 10Å are highlighted. The number of occurrences of interactions for each residue across all six structures was summed to yield the hot spot score. A heatmap produced from the hot spot scores, with scaling based on the number of interactions for a given residue, was used to color the Ub structure in Figure 4.

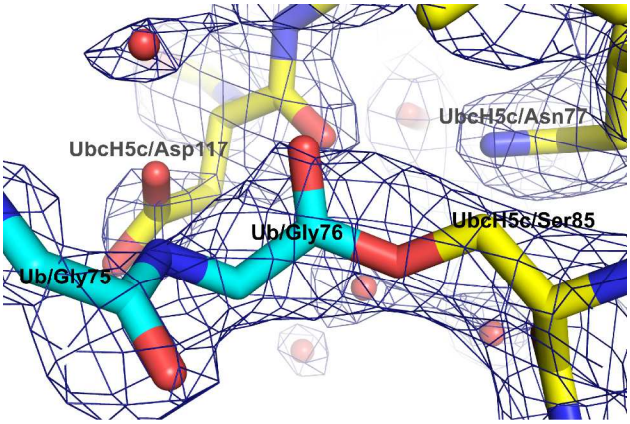

Supplemental Figure S2. A closeup view of the oxyester bond between UbcH5c-Ser85 and Ub-Gly76. A $2F_o$-F_c electron density map (dark blue) from the final refinement is contoured at 1.2σ.

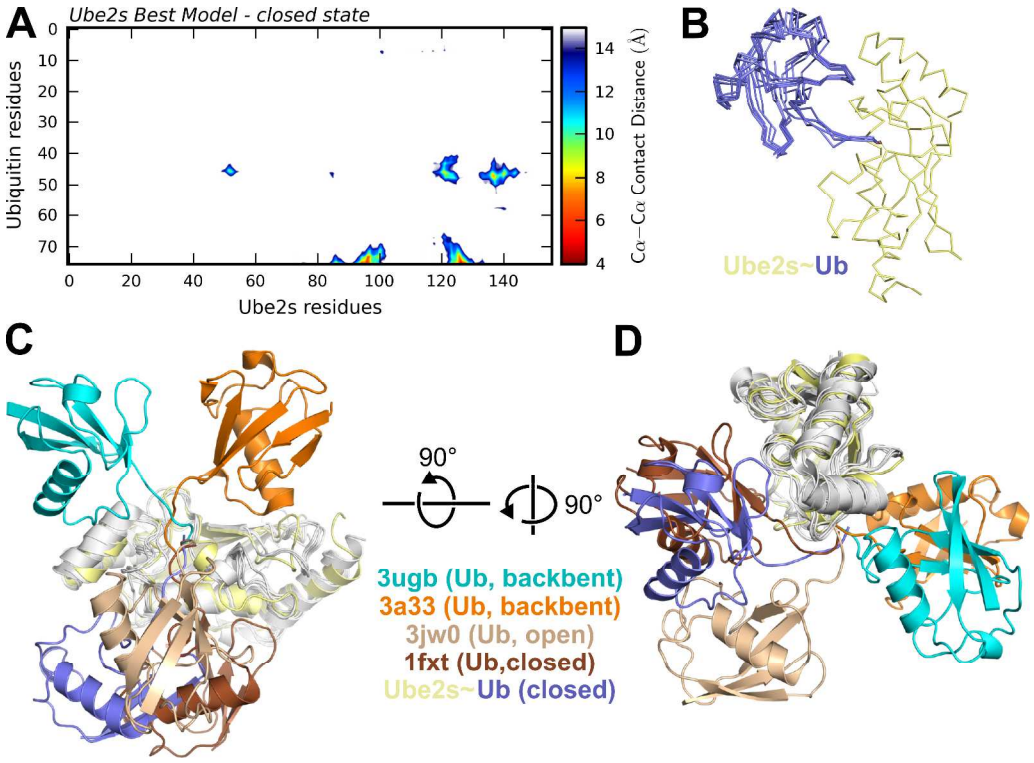

Supplemental Figure S3. Cα-Cα contact distance plot and Ub orientation for the Ube2s~Ub conjugate model. (A) Cα-Cα contact distance plot of Ube2s~Ub residue pairs separated by a distance of 15 Å or less. (B) Alignment of the five best molecular models for the Ube2s~Ub conjugate. Ube2s (yellow) and Ub (blue) are shown as a ribbon representation with all structures aligned using Ube2s residues 6-156. (C) Alignment of the best Ube2s~Ub model (Ube2s: yellow, Ub: blue) with the E2~Ub conjugates PDB 3ugb (UbcH5c:gray, Ub:cyan), PDB 3a33 (UbcH5b:gray, Ub:orange) (*15*), PDB 3jw0 (UbcH5b:gray, Ub:wheat) (*16*) and PDB 1fxt (Ubc1:gray, Ub:brown) (*17*). (D) Structural alignment in (C) with a 90° rotation about the x-axis followed by a 90° rotation about the y-axis.

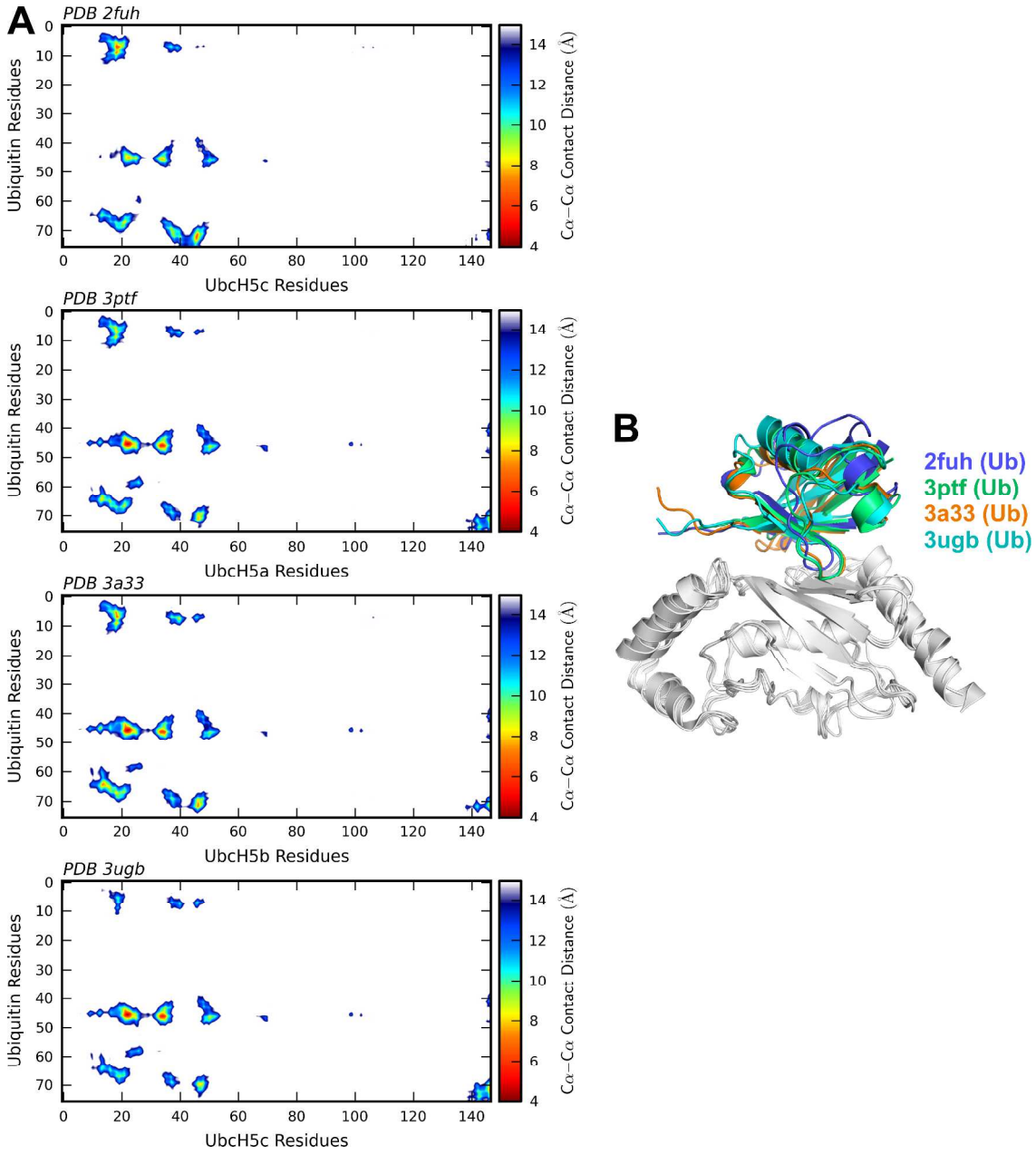

Supplemental Figure S4. The canonical UbcH5/Ub backside interaction is observed in multiple structures deposited in the PDB. (A) Cα-Cα contact distance plots for PDB 2fuh (UbcH5c/Ub noncovalent complex NMR structure) (*18*), PDB 3ptf (UbcH5a/Ub noncovalaent complex crystal structure) (*19*), PDB 3a33 (UbcH5b/Ub noncovalent interaction within the UbcH5b~Ub infinite spiral conjugate oligomer) (*15*) and PDB 3ugb (UbcH5c/Ub noncovalent interaction within the UbcH5c~Ub linear staggered oligomer) indicate a nearly identical pattern of contact residues which mediate the UbcH5/Ub backside interaction. (B) The positioning of ubiquitin chains participating in backside contact with UbcH5 are nearly identical for PDB 2fuh (UbcH5c: white and Ub: blue), PDB 3ptf (UbcH5a: white and Ub: green), PDB 3a33 (UbcH5b: white and Ub: orange) and PDB 3ugb (UbcH5c: white and Ub: cyan).

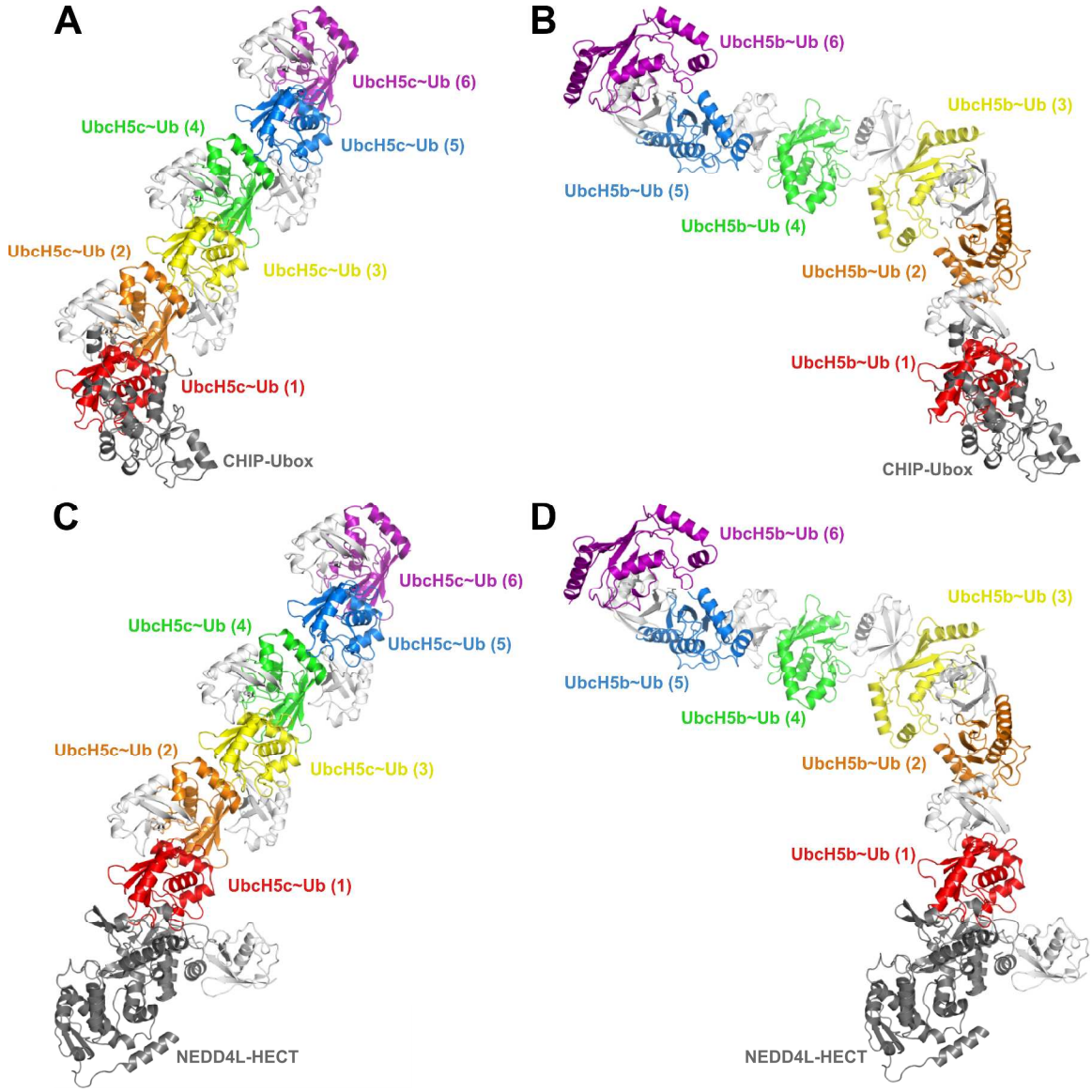

Supplemental Figure S5. Models of UbcH5~Ub staggered linear and infinite spiral oligomers with Ubox and HECT domains. (A) Docked model of the CHIP-Ubox in complex with the staggered linear array UbcH5c~Ub conjugate oligomer. (B) Docked model of the CHIP-Ubox in complex with the infinite spiral UbcH5b~Ub conjugate oligomer. (C) Docked model of the NEDD4L-HECT in complex with the staggered linear array UbcH5c~Ub conjugate oligomer. (D) Docked model of the NEDD4L-HECT in complex with the infinite spiral UbcH5b~Ub conjugate oligomer. Docking of the initiating E2~Ub to the CHIP-Ubox was carried out by aligning UbcH5c from PDB 3ugb and UbcH5b from PDB 3a33 onto the UbcH5a molecule of PDB ID 2oxq (*11*). Docking of the initiating E2~Ub to the NEDD4L-HECT was carried out by aligning UbcH5c from PDB 3ugb and UbcH5b from PDB 3a33 onto the UbcH5b molecule of PDB ID 3jw0 (*16*).

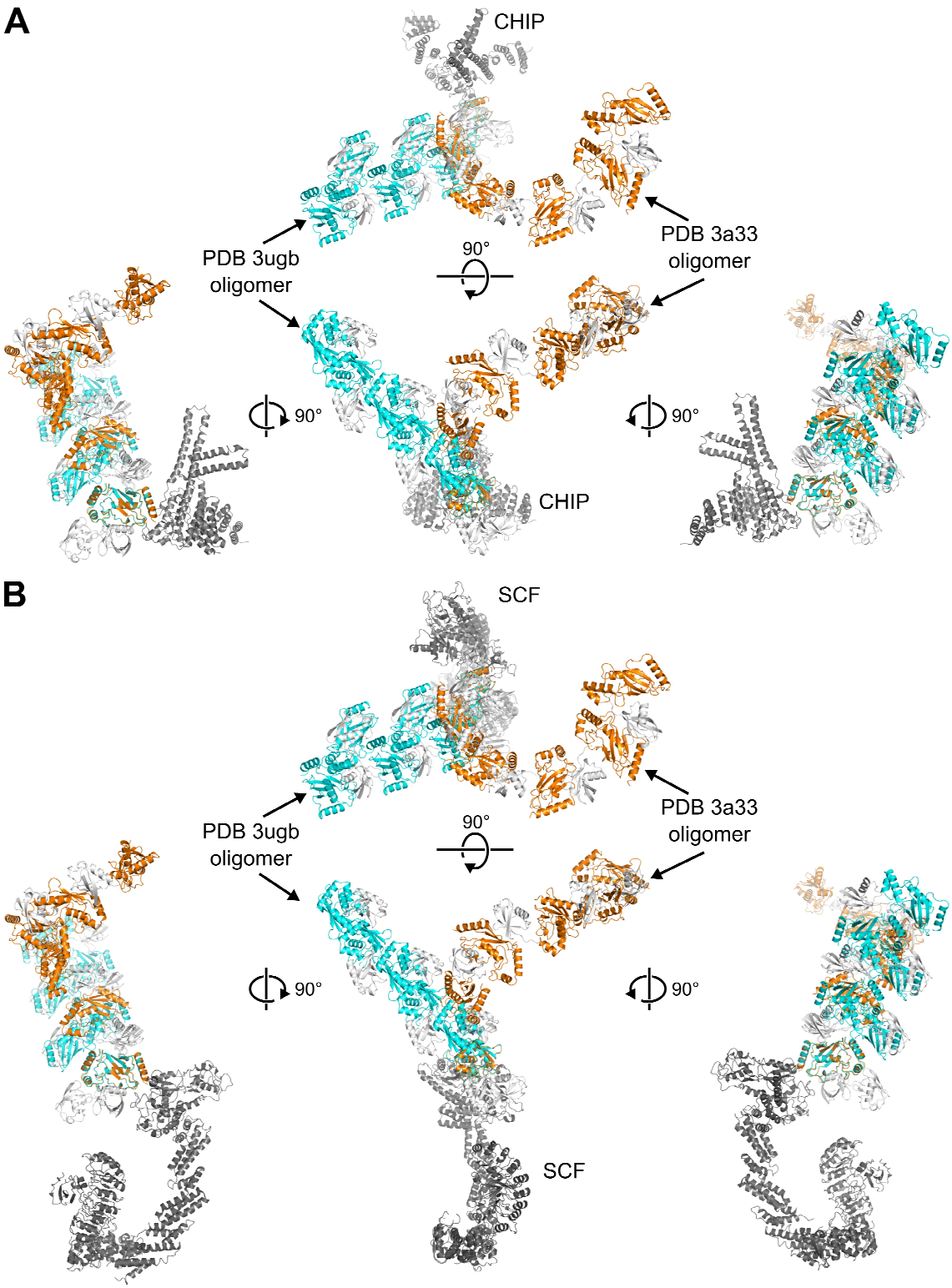

Supplemental Figure S6. Models of UbcH5~Ub conjugate oligomers with the full length CHIP and the Cul1-Rbx1-Skp1-Skp2 SCF ligase complex. (A) Docked models of complexes between the infinite linear staggered UbcH5c~Ub oligomer from PDB 3ugb

(UbcH5c: cyan and Ub: white) or the infinite spiral UbcH5b~Ub oligomer from PDB 3a33 (UbcH5b: orange and Ub: white) and the E3 enzyme CHIP (grey). (B) Docked models of complexes between the infinite linear staggered UbcH5c~Ub oligomer from PDB 3ugb (UbcH5c: cyan and Ub: white) or the infinite spiral UbcH5b~Ub oligomer from PDB 3a33 (UbcH5b: orange and Ub: white) and the E3 enzyme CHIP (grey). Rotation axes are shown throughout to illustrate transformation between the center complex and the rotated views.

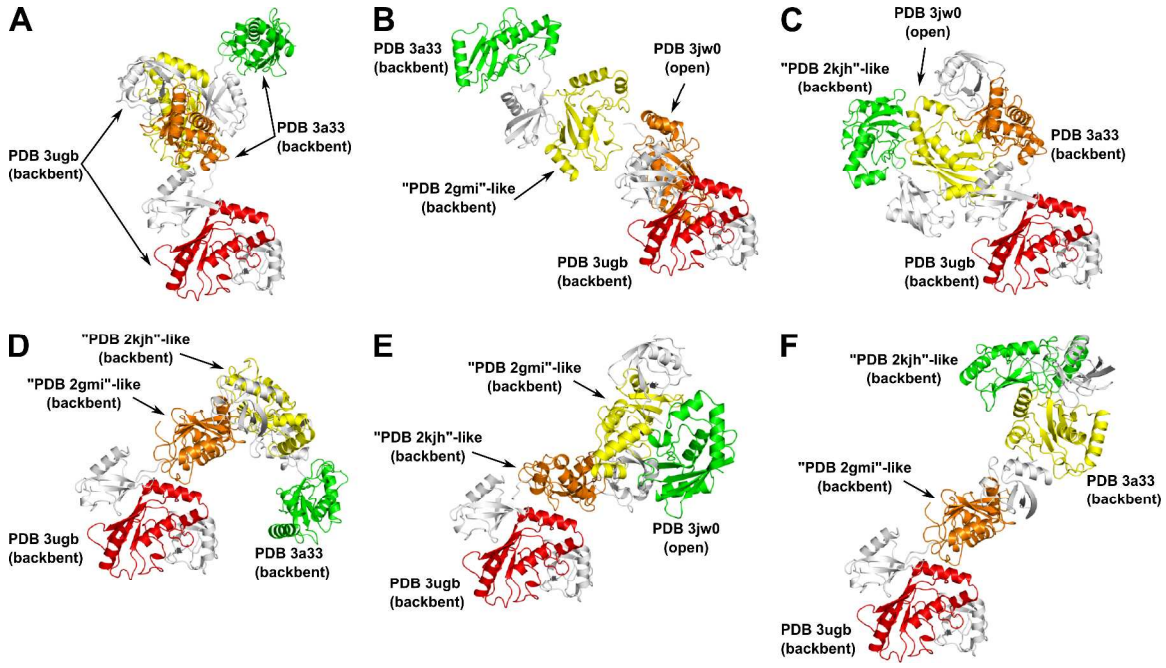

Supplemental Figure S7. Structural variability and diversity of E2~Ub oligomers. (A) One example of a mixed architecture UbcH5~Ub oligomer comprised of four UbcH5~Ub conjugates using E2~Ub coordinates from PDB 3a33 (UbcH5b~Ub) and PDB 3ugb (UbcH5c~Ub). (B-F) Examples for 5 of the 125 possible isomers for an oligomer chain of four UbcH5~Ub conjugates using UbcH5~Ub orientations similar to those observed in PDB 2gmi ("PDB 2gmi"-like), PDB 2kjh ("PDB 2kjh"-like) in combination with those observed in PDB 3a33 (UbcH5b~Ub), PDB 3jw0 (UbcH5b~Ub) and PDB 3ugb (UbcH5c~Ub). Throughout the figure, all Ub molecules are colored white, the first UbcH5 is red, the second is orange, the third UbcH5 is yellow and the fourth UbcH5 is green. Each UbcH5~Ub conjugate is labeled with a description of the intra-conjugate Ub orientation.

SUPPLEMENTAL TABLES

Supplemental Table S1. Solvent accessibility of the E2~Ub conjugate bond and surrounding active site residues.

E2~Ub Structure	Solvent Accessibility (Å^2)[a] E2~Ub conjugate bond[b]
PDB 1fxt	11.40
PDB 2gmi	11.07
PDB 2kjh	24.32 (14.36[c])
PDB 3a33	13.15
PDB 3jw0	5.37
PDB 3ugb	6.26
Ube2s~Ub model[d]	6.13
Average (stabilized)[e]	12.50
Average (activated)[f]	5.92

[a] Per residue solvent accessible surface area (SASA) calculated by the *WHAT IF* webserver (*20*).
[b] The E2~Ub conjugate bond is defined as the residues of the E2 active site Cys/Ser and Ub-Gly76.
[c] Solvent accessibility not including the side chain of Ub-Cys76.
[d] The best Ube2s~Ub model was used for solvent accessible surface area calculations.
[e] Average SASA for structures PDB 1fxt (*17*), PDB 2gmi (*21*), PDB 2kjh (*22*) and PDB 3a33 (*15*) (not including the PDB 2kjh Ub-Cys76 side chain).
[f] Average SASA for structures PDB 3jw0 (*16*), PDB 3ugb and the best Ube2s~Ub model.

Supplemental References

1. de Vries, S. J., van Dijk, A. D., Krzeminski, M., van Dijk, M., Thureau, A., Hsu, V., Wassenaar, T., and Bonvin, A. M. (2007) HADDOCK versus HADDOCK: new features and performance of HADDOCK2.0 on the CAPRI targets, *Proteins 69*, 726-733.
2. Wickliffe, K. E., Lorenz, S., Wemmer, D. E., Kuriyan, J., and Rape, M. (2011) The mechanism of linkage-specific ubiquitin chain elongation by a single-subunit E2, *Cell 144*, 769-781.
3. Clore, G. M., and Schwieters, C. D. (2003) Docking of protein-protein complexes on the basis of highly ambiguous intermolecular distance restraints derived from 1H/15N chemical shift mapping and backbone 15N-1H residual dipolar couplings using conjoined rigid body/torsion angle dynamics, *J Am Chem Soc 125*, 2902-2912.
4. Kumar, S., and Nussinov, R. (2002) Relationship between ion pair geometries and electrostatic strengths in proteins, *Biophys J 83*, 1595-1612.
5. Xu, D., Tsai, C. J., and Nussinov, R. (1997) Hydrogen bonds and salt bridges across protein-protein interfaces, *Protein Eng 10*, 999-1012.
6. Clore, G. M., and Kuszewski, J. (2002) Chi(1) rotamer populations and angles of mobile surface side chains are accurately predicted by a torsion angle database potential of mean force, *J Am Chem Soc 124*, 2866-2867.
7. Cock, P. J., Antao, T., Chang, J. T., Chapman, B. A., Cox, C. J., Dalke, A., Friedberg, I., Hamelryck, T., Kauff, F., Wilczynski, B., and de Hoon, M. J. (2009) Biopython: freely available Python tools for computational molecular biology and bioinformatics, *Bioinformatics 25*, 1422-1423.

8. Chen, V. B., Arendall, W. B., 3rd, Headd, J. J., Keedy, D. A., Immormino, R. M., Kapral, G. J., Murray, L. W., Richardson, J. S., and Richardson, D. C. (2010) MolProbity: all-atom structure validation for macromolecular crystallography, *Acta Crystallogr D Biol Crystallogr 66*, 12-21.
9. Davis, I. W., Leaver-Fay, A., Chen, V. B., Block, J. N., Kapral, G. J., Wang, X., Murray, L. W., Arendall, W. B., 3rd, Snoeyink, J., Richardson, J. S., and Richardson, D. C. (2007) MolProbity: all-atom contacts and structure validation for proteins and nucleic acids, *Nucleic Acids Res 35*, W375-383.
10. Zhang, M., Windheim, M., Roe, S. M., Peggie, M., Cohen, P., Prodromou, C., and Pearl, L. H. (2005) Chaperoned ubiquitylation--crystal structures of the CHIP U box E3 ubiquitin ligase and a CHIP-Ubc13-Uev1a complex, *Mol Cell 20*, 525-538.
11. Xu, Z., Kohli, E., Devlin, K. I., Bold, M., Nix, J. C., and Misra, S. (2008) Interactions between the quality control ubiquitin ligase CHIP and ubiquitin conjugating enzymes, *BMC Struct Biol 8*, 26.
12. Zheng, N., Schulman, B. A., Song, L., Miller, J. J., Jeffrey, P. D., Wang, P., Chu, C., Koepp, D. M., Elledge, S. J., Pagano, M., Conaway, R. C., Conaway, J. W., Harper, J. W., and Pavletich, N. P. (2002) Structure of the Cul1-Rbx1-Skp1-F boxSkp2 SCF ubiquitin ligase complex, *Nature 416*, 703-709.
13. Hao, B., Zheng, N., Schulman, B. A., Wu, G., Miller, J. J., Pagano, M., and Pavletich, N. P. (2005) Structural basis of the Cks1-dependent recognition of p27(Kip1) by the SCF(Skp2) ubiquitin ligase, *Mol Cell 20*, 9-19.
14. Zheng, N., Wang, P., Jeffrey, P. D., and Pavletich, N. P. (2000) Structure of a c-Cbl-UbcH7 complex: RING domain function in ubiquitin-protein ligases, *Cell 102*, 533-539.
15. Sakata, E., Satoh, T., Yamamoto, S., Yamaguchi, Y., Yagi-Utsumi, M., Kurimoto, E., Tanaka, K., Wakatsuki, S., and Kato, K. (2010) Crystal structure of UbcH5b~ubiquitin intermediate: insight into the formation of the self-assembled E2~Ub conjugates, *Structure 18*, 138-147.
16. Kamadurai, H. B., Souphron, J., Scott, D. C., Duda, D. M., Miller, D. J., Stringer, D., Piper, R. C., and Schulman, B. A. (2009) Insights into ubiquitin transfer cascades from a structure of a UbcH5B approximately ubiquitin-HECT(NEDD4L) complex, *Mol Cell 36*, 1095-1102.
17. Hamilton, K. S., Ellison, M. J., Barber, K. R., Williams, R. S., Huzil, J. T., McKenna, S., Ptak, C., Glover, M., and Shaw, G. S. (2001) Structure of a conjugating enzyme-ubiquitin thiolester intermediate reveals a novel role for the ubiquitin tail, *Structure 9*, 897-904.
18. Brzovic, P. S., Lissounov, A., Christensen, D. E., Hoyt, D. W., and Klevit, R. E. (2006) A UbcH5/ubiquitin noncovalent complex is required for processive BRCA1-directed ubiquitination, *Mol Cell 21*, 873-880.
19. Bosanac, I., Phu, L., Pan, B., Zilberleyb, I., Maurer, B., Dixit, V. M., Hymowitz, S. G., and Kirkpatrick, D. S. (2011) Modulation of K11-linkage formation by variable loop residues within UbcH5A, *J Mol Biol 408*, 420-431.
20. Vriend, G. (1990) WHAT IF: a molecular modeling and drug design program, *J Mol Graph 8*, 52-56, 29.

21. Eddins, M. J., Carlile, C. M., Gomez, K. M., Pickart, C. M., and Wolberger, C. (2006) Mms2-Ubc13 covalently bound to ubiquitin reveals the structural basis of linkage-specific polyubiquitin chain formation, *Nat Struct Mol Biol 13*, 915-920.
22. Serniwka, S. A., and Shaw, G. S. (2009) The structure of the UbcH8-ubiquitin complex shows a unique ubiquitin interaction site, *Biochemistry 48*, 12169-12179.